



In accord with methods pioneered by Sauvage and co-workers,<sup>[4b,c]</sup> simple mixing of **3**, **4**, and  $\text{Cu}^{1+}$  or  $\text{Zn}^{2+}$  ions produces metallorotaxane monomers **1** and **2** (Scheme 1). Controlled oxidation results in the electropolymerization of the macrocycle **4**, while leaving the threading group **3** untouched. Higher potentials can be subsequently applied to polymerize **3**. The detailed procedure is as follows: Microelectrode arrays<sup>[8]</sup> were immersed in a solution (0.1 M  $n\text{Bu}_4\text{NPF}_6$ ,  $\text{CH}_2\text{Cl}_2$ ) of **1**, **2**, or **4** (0.3 mM) and then cycled between  $-0.5$  and  $0.55$  V versus ferrocene/ferrocenium ( $\text{Fc}/\text{Fc}^+$ ). This procedure results in the oxidative electropolymerization of the macrocycle to produce poly**1**, poly**2**, and poly**4**. Consistent with the proposed polymerization, cyclic voltammograms of poly**2** in fresh monomer-free electrolyte gave voltammograms indistinguishable from those obtained from poly**4**. The cyclic voltammogram of poly**1** (Figure 1) is also similar but contains an added  $\text{Cu}^{1+}/\text{Cu}^{2+}$  wave centered at  $0.11$  V vs.  $\text{Fc}/\text{Fc}^+$ . The UV/Vis spectra also support the selective polymerization of the macrocyclic ligand, and both poly**1** and poly**2** displayed absorption spectra similar to that of poly**4** ( $\lambda_{\text{max}} = 503$  nm) with an additional absorption feature at about  $450$  nm assigned to the threading ligand **3**.

Subjecting deposited films of poly**1** or poly**2** to higher potentials in monomer-free electrolyte resulted in the polymerization of the 4,4'-bis(dithienyl)-2,2'-bipyridine threading

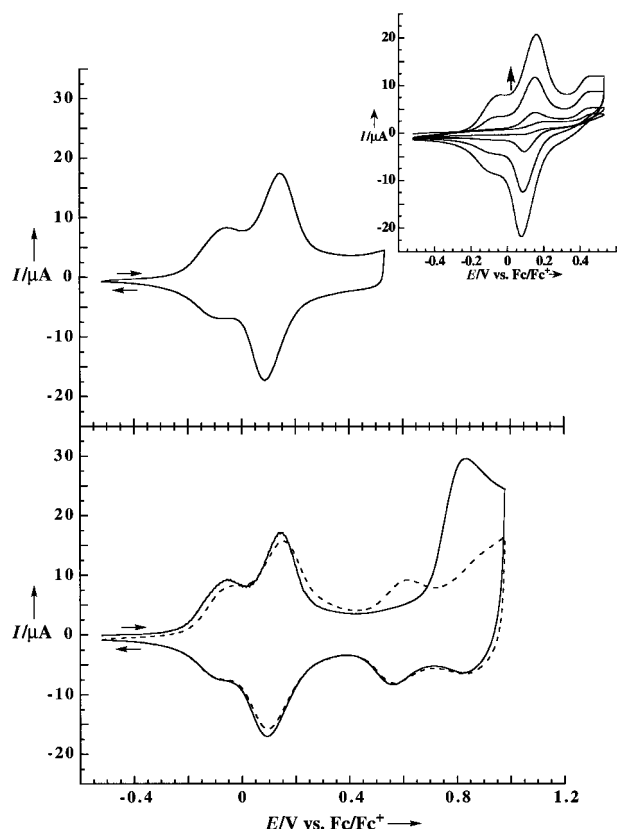


Figure 1. Cyclic voltammograms of **1**, poly**1**, and poly**1-L** on interdigitated microelectrodes with a spacing of  $5 \mu\text{m}$  between adjacent electrodes (0.1 M  $(n\text{Bu}_4\text{N})\text{PF}_6$  in  $\text{CH}_2\text{Cl}_2$  at a sweep rate of  $100 \text{ mV s}^{-1}$ ). Top: A film of poly**1** in fresh, monomer-free electrolyte. Inset: The first electropolymerization to grow films of poly**1** after 1, 20, 40, and 60 potential cycles. Bottom: The first scan (solid line) and second scan (dashed line) of the same film when swept to  $1.0$  V vs.  $\text{Fc}/\text{Fc}^+$ . The first scan shows the large irreversible oxidation to form poly**1-L**.

ligand to form ladder polymers poly**1-L** and poly**2-L**, respectively (Scheme 1). This process is readily apparent from Figure 1, wherein the first sweep to  $1$  V vs.  $\text{Fc}/\text{Fc}^+$  results in a large irreversible oxidation current. This irreversible current is expected since oxidation of the threading ligand **3** will produce radical cations that undergo intermolecular coupling with loss of protons to form new thiophene–thiophene linkages (i.e., polymerization). The second sweep over the same expanded potential range lacks this irreversible oxidation and is identical to all subsequent sweeps.

The efficiency of the second polymerization can be deduced from an analysis of the irreversible charge relative to the reversible charge. A key parameter is the mass of the polymer immobilized on the electrodes. Once the mass of the polymer has been determined, the degree of oxidation of the polymer is also known. This analysis was afforded by a comparison of poly**1**, poly**2**, and poly**4**. Due to the fact that the metal ions do not directly interact with the electronic structure of the macrocyclic polymer, poly**2** and poly**4** have nearly identical cyclic voltammograms over the potential region of  $-0.5$  to  $0.55$  V vs.  $\text{Fc}/\text{Fc}^+$ , and display the same number of Coulombs per gram of polymer deposited. Polymer poly**1** has an additional one-electron  $\text{Cu}^{1+}/\text{Cu}^{2+}$  wave in that potential region, which also serves as an internal standard to establish the moles of polymer repeating units in the film.

We find that poly**1**, poly**2**, and poly**4** are respectively oxidized by 3.2, 2.2, and 2.2 electrons per repeating unit when cycled to  $0.55$  V vs.  $\text{Fc}/\text{Fc}^+$ . With regard to the efficiency of the second polymerization of poly**1** and poly**2**, the respective irreversible charge passed was 1.7 and 2.1 electrons per repeating group. A quantitative polymerization results in two electrons per monomer being removed irreversibly. Hence the second polymerization is quantitative for poly**2**, whereas for poly**1** it appears that some loss of the threading ligand **3** and the Cu ion occurs. The lower stability of the Cu complex is not unexpected, since at higher potential the  $\text{Cu}^{2+}$  ion generated would prefer to be five-coordinate, which is not easily accommodated by the rotaxane structure. After the first sweep to high potential a stable reproducible voltammogram is observed, and with application of  $0.98$  V vs.  $\text{Fc}/\text{Fc}^+$  5.3, 5.4, and 3.3 electrons per repeating unit were removed for poly**1-L**, poly**2-L**, and poly**4**, respectively. For a perfect structure we would expect that poly**1-L**, due to the presence of Cu ion, would be oxidized by one more electron than poly**2-L**. The smaller value for poly**1-L** reflects the concurrent loss of **3** and the Cu ion. The two-electron difference between poly**2-L** and poly**3** is also consistent with our previous investigations that demonstrated the two high potential waves ( $+0.6$  and  $+0.85$  V vs.  $\text{Fc}/\text{Fc}^+$ ) are one-electron oxidations of the tetrathienyl segments.<sup>[5, 6, 9]</sup>

The linear dimensions of the two polymerizable groups and the structure of the metallorotaxane were chosen to promote the formation of a three-stranded ladder polymer (Scheme 1). Neglecting minor effects arising from conformational issues (there are two enantiomeric conformations of **1** and **2**) the polymer formed from the threading unit is twice as long as the polymer containing the macrocycle. Additionally, computationally optimized structures<sup>[10]</sup> of the monomers indicate that the two polymerizable groups are rigidly held in a parallel

orientation. These structural features and the polymerization of the threading ligand require the structure of the polymer to contain a predominance of the three-stranded ladder architecture shown in Scheme 1. The data does not preclude the presence of cross-links, and it is likely that the structure contains defects. This ladder polymer structure is of particular interest due to the fact that the macrocyclic-containing polymer (poly4) is sandwiched between two chains for poly3. In other words, we have in essence assembled a three-stranded molecular wire in which the internal wire is encapsulated between two polymer chains.

To further illustrate the viability of this structure, we have conducted molecular mechanics calculations on oligomers assembled from the computationally optimized monomer.<sup>[10]</sup> In these calculations a single enantiomer of **1** was used. As can be seen from the space-filling structure shown in Figure 2, there is a clear match of the polymer lengths, and the chain of poly4 is incarcerated between two strands of poly3. An additional feature revealed by the structure is the steric constraints of the phenanthroline portion of the macrocycle. This unit presents a rigid steric barrier that prevents close contacts between neighboring polymers and thereby promotes intrapolymer coupling in the second polymerization to favor the three-strand ladder structure.

Comparisons of the conductivity and electrochemistry of poly1-L, poly2-L, and poly4 (Figure 3) support our assertion that the internal polymer behaves as a partially isolated wire when the outer two polymer strands are in their insulating (undoped) state. The observed electroactivity results from

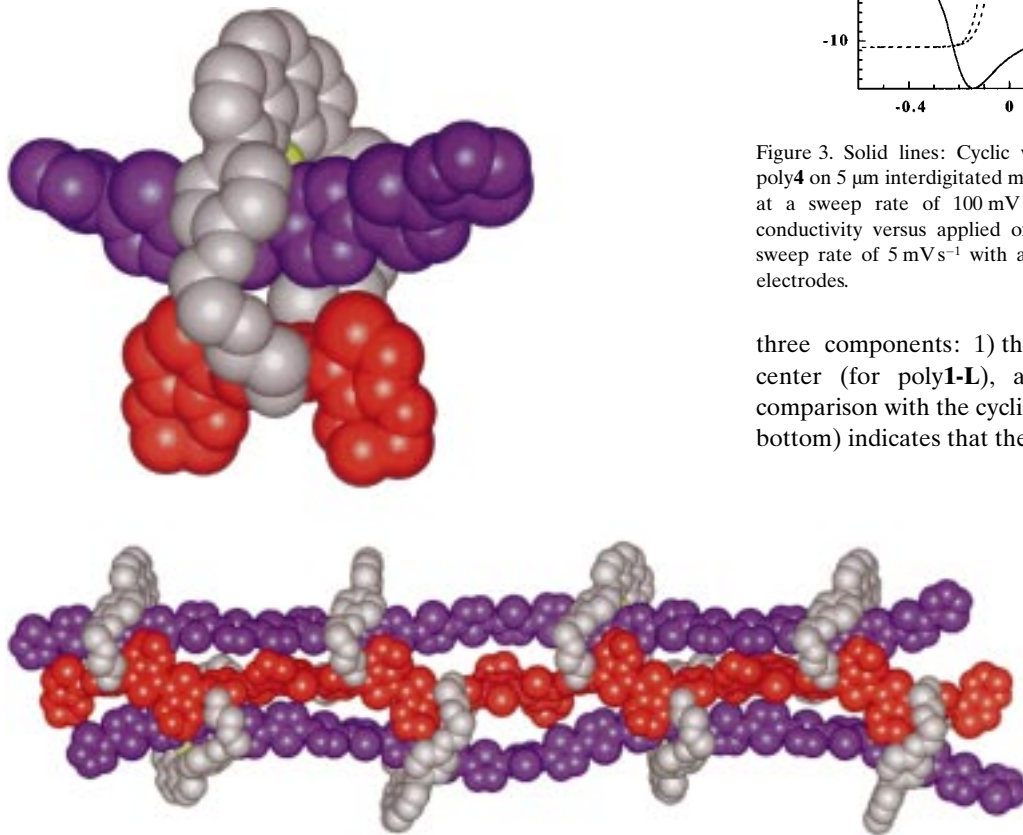


Figure 2. Space-filling model of **1** (top) and an octamer of poly1-L (bottom). The backbone of poly4 is shown in red, the diethylene glycol chains and the phenanthroline portion of the macrocycle are shown in gray, and the poly3 chains are shown in purple.

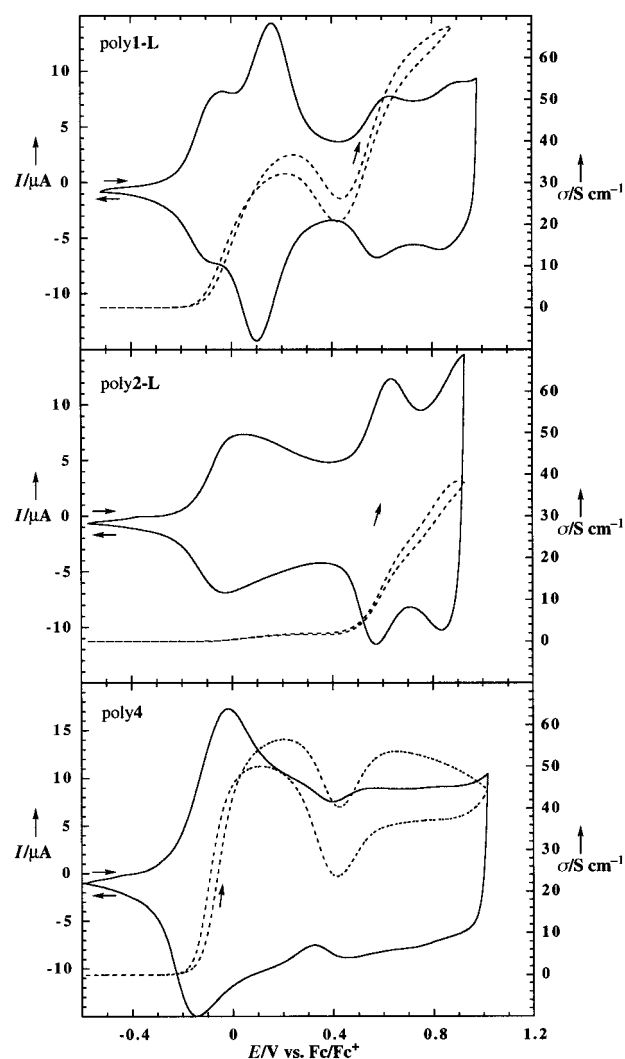
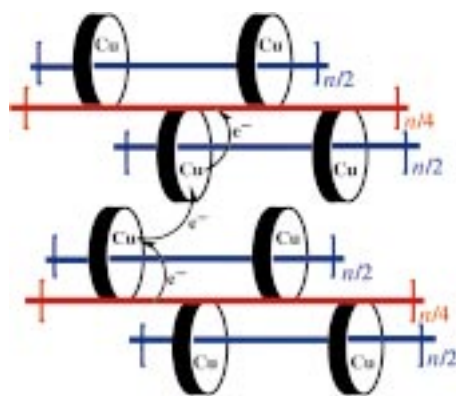


Figure 3. Solid lines: Cyclic voltammograms of poly1-L, poly2-L, and poly4 on 5  $\mu\text{m}$  interdigitated microelectrodes (0.1M  $(n\text{Bu}_4\text{N})\text{PF}_6$  in  $\text{CH}_2\text{Cl}_2$  at a sweep rate of  $100\text{ mV s}^{-1}$ ). Dashed lines: Plots of the in situ conductivity versus applied oxidation potential of the same films at a sweep rate of  $5\text{ mV s}^{-1}$  with a 40 mV offset potential between adjacent electrodes.

three components: 1) the macrocyclic polymer, 2) the Cu center (for poly1-L), and 3) the threading polymer. A comparison with the cyclic voltammogram of poly4 (Figure 3, bottom) indicates that the first wave at about 0.1 V vs.  $\text{Fc}/\text{Fc}^+$  and a broad featureless wave for electroactivity at more positive potentials than for poly1-L and poly2-L can be assigned to the macrocycle-containing polymer. For poly1-L the  $\text{Cu}^{\text{I+}}/\text{Cu}^{\text{2+}}$  wave overlaps the wave for electroactivity of the macrocyclic polymer, which creates an optimal situation for the Cu-centered electroactivity to enhance the conductivity.

The conductivities of rotaxane complexes of poly3 have

been previously determined to be low (ca.  $10^{-3} \text{ Scm}^{-1}$ ), and thus the poly4 backbone is the dominant contributor to the conductivity of the ladder polymers. Simple inspection of Figure 2 reveals that the conductivity of poly1-L<sup>[11]</sup> ( $\sigma$ ) at 0.25 V vs. Fc/Fc<sup>+</sup> is  $38 \text{ Scm}^{-1}$ , approximately 20 times higher than for poly2-L at the same potential ( $\sigma = 2 \text{ Scm}^{-1}$ ); the conductivity of poly4 at the same potential is  $66 \text{ Scm}^{-1}$ . All three materials poly1-L, poly2-L, and poly4 display comparable (within a factor of 2) conductivities at high potentials ( $\approx 0.9 \text{ V vs. Fc/Fc}^+$ ). These comparisons of conductivity demonstrate that the central macrocyclic polymer (poly4) in poly1-L and poly2-L is isolated by the outer polymers (poly3 chains) when they are in their insulating states. When the poly3 chains are insulating, the electroactivity of the Cu ions can assist in interchain transport. We had previously determined that the conductivity of polymers is enhanced when the wave for electroactivity of a metal center overlaps that of the conjugated polymer.<sup>[5b, 12]</sup> Based upon these previous studies the redox potential of the Cu ion is optimally positioned to participate in the conduction. This effect, illustrated in Scheme 2, is responsible for the much larger conductivity at



Scheme 2. Schematic representation of the participation of the Cu ion in the conduction.

lower potentials of poly1-L relative to poly2-L. In the absence of a rotaxane structure the polymer chains of poly3 can come in close proximity, and poly4 exhibits a high conductivity without the Cu-centered electroactivity. At higher potentials the poly3 chains are redox-active and mediate interchain conduction. Hence, we have similar conductivities for poly1-L, poly2-L, and poly4.

We have demonstrated a powerful new approach for the assembly of conducting three-strand ladder polymers. By design, we have produced a noncovalent ladder polymer that encloses a central polymer in a sandwich structure between two other polymers. The three-strand structure may be extended to create supramolecular structures wherein a central polymer is protected between two inert insulating polymers. Such an approach may prove important in the quest for insulated metallic molecular wires and also provides a novel mechanism for the formation of high stability conjugated polymers. The dramatic effect of the copper ion on the conductivity also suggests that similar processes may be of use for the design of chemoresistive sensory materials.

### Experimental Section

General procedures: Reactions were carried out in oven-dried glassware using standard Schlenk techniques under an inert atmosphere of dry argon. <sup>1</sup>H NMR spectra were recorded with a Bruker AC-250 or Varian Inova-500 MHz spectrometers. Electrochemical measurements were performed in an air-free dry-box using a computer-controlled Autolab Model PGSTAT 20 potentiostat from Eco Chemie. All electrochemical measurements were performed on interdigitated array microelectrodes purchased from AAI-ABTECH with an interelectrode spacing of 5  $\mu\text{m}$ , with a platinum coil counterelectrode and an isolated Ag wire quasi-reference electrode. All potentials are reported versus the Fc/Fc<sup>+</sup> redox couple. Compound 6 was synthesized from the tosylate<sup>[14]</sup> by simple exchange with iodide ion, and 7 was prepared as reported previously.<sup>[15]</sup> Macrocycle 5 was produced by straightforward adaptation of conditions used for the synthesis of related macrocycles.<sup>[15]</sup>

**4:** Compound 5 (100 mg, 0.115 mmol), 2-(tributylstannyl)-3,4-ethylene-dioxythiophene (124 mg, 0.288 mmol), CuI (66 mg, 0.346 mmol), and *trans*-[PdCl<sub>2</sub>(PPh<sub>3</sub>)<sub>2</sub>] (4 mg) were dissolved in dry DMF (10 mL), and the mixture was stirred overnight at 80 °C. The DMF was then evaporated, and the residue was extracted with CH<sub>2</sub>Cl<sub>2</sub>/NH<sub>4</sub>OH. The organic phase was dried, and the crude product was precipitated with hexane. Column chromatography (SiO<sub>2</sub>, CH<sub>2</sub>Cl<sub>2</sub>/MeOH 99/1) afforded the desired compound as a yellow solid in 90% yield. <sup>1</sup>H NMR (500 MHz, CDCl<sub>3</sub>):  $\delta$  = 3.98 (m, 4H), 4.02 (m, 4H), 4.11 (m, 4H), 4.23 (m, 8H), 4.31 (m, 4H), 6.40 (s, 2H), 7.07 (d,  $J$  = 8.0 Hz, 4H), 7.74 (s, 2H), 7.81 (s, 2H), 8.07 (d,  $J$  = 8.2 Hz, 2H), 8.26 (d,  $J$  = 8.2 Hz, 2H), 8.39 (d,  $J$  = 8.0 Hz, 4H); HR-MS (FAB): calcd for C<sub>50</sub>H<sub>42</sub>N<sub>2</sub>O<sub>10</sub>S<sub>2</sub> [M+H]<sup>+</sup>: 895.2359, found: 895.2346.

**Monomer 1:** A solution of [Cu(MeCN)<sub>4</sub>]BF<sub>4</sub> (5.3 mg, 0.017 mmol) in dry deoxygenated MeCN (2 mL) was transferred through a cannula to a solution of 3 (8 mg, 0.017 mmol) and 4 (15 mg, 0.017 mmol) in dry deoxygenated CH<sub>2</sub>Cl<sub>2</sub> (10 mL). After 3 h stirring the solvents were evaporated, and the residue was dissolved in acetone and filtered. Concentration and addition of diethyl ether afforded compound 1 as a green powder that was isolated in 60% yield. <sup>1</sup>H NMR (500 MHz, [D<sub>6</sub>]acetone):  $\delta$  = 3.79, 3.9, 4.05, 4.18, 4.29, 4.38, 4.69 (m, 24H), 6.30 (d,  $J$  = 8.8 Hz, 4H), 6.61 (s, 2H), 7.14 (dd,  $J$  = 5.2, 5.2 Hz, 2H), 7.30 (m, 4H), 7.36 (dd,  $J$  = 3.7, 1.2 Hz, 2H), 7.39 (d,  $J$  = 4.0 Hz, 2H), 7.51 (dd,  $J$  = 5.2, 1.2 Hz, 2H), 7.64 (d,  $J$  = 8.5 Hz, 4H), 7.79 (dd,  $J$  = 8.5, 2.4 Hz, 2H), 8.18 (s, 2H), 8.26 (d,  $J$  = 2.1 Hz, 2H), 8.29 (d,  $J$  = 8.2 Hz, 2H), 8.31 (s, 2H), 8.89 (d,  $J$  = 8.2 Hz, 2H); HR-MS (FAB): calcd for C<sub>76</sub>H<sub>58</sub>N<sub>4</sub>O<sub>10</sub>S<sub>6</sub>Cu [M+H]<sup>+</sup>: 1442.1851, found: 1442.1878.

**Monomer 2:** The synthesis was performed as described for 1, using [Zn(ClO<sub>4</sub>)<sub>2</sub>]·6H<sub>2</sub>O (4.2 mg, 0.01 mmol), 3 (5.4 mg, 0.01 mmol), and 4 (10 mg, 0.01 mmol). The product was isolated in 90% yield as an orange solid. <sup>1</sup>H NMR (500 MHz, [D<sub>6</sub>]acetone):  $\delta$  = 3.70, 3.88, 3.93, 4.04, 4.16, 4.29, 4.40, 4.67 (m, 24H), 6.52 (d,  $J$  = 9.0 Hz, 4H), 6.67 (s, 2H), 7.16 (dd,  $J$  = 5.0, 5.0 Hz, 2H), 7.33 (d,  $J$  = 4.0 Hz, 4H), 7.37 (dd,  $J$  = 3.5, 1.2 Hz, 2H), 7.42 (d,  $J$  = 4.0 Hz, 2H), 7.53 (d,  $J$  = 8.5 Hz, 2H), 7.56 (dd,  $J$  = 5.2, 1.2 Hz, 2H), 7.59 (d,  $J$  = 8.5 Hz, 4H), 7.87 (dd,  $J$  = 8.5, 2.5 Hz, 2H), 8.15 (s, 2H), 8.39 (m, 2H), 8.44 (d,  $J$  = 8.5 Hz, 2H), 8.49 (s, 2H), 9.18 (d,  $J$  = 8.5 Hz, 2H); HR-MS (FAB): calcd for C<sub>76</sub>H<sub>58</sub>N<sub>4</sub>O<sub>10</sub>S<sub>6</sub>Zn [M+H]<sup>+</sup>: 1443.1846, found: 1443.1873.

Received: August 30, 1999 [Z13941]

- [1] S. M. Sze, *The Physics of Semiconductor Devices*, 2nd ed., Wiley, New York, 1981.
- [2] P. K. H. Ho, D. S. Thomas, R. H. Friend, N. Tessler, *Science* 1999, 285, 233.
- [3] *Comprehensive Supramolecular Chemistry*, Vols. 1–10 (Eds.: J. L. Atwood, J. D. D. Davies, D. D. MacNicol, F. Vögtle), Pergamon, New York, 1996.
- [4] a) F. M. Raymo, J. F. Stoddart, *Chem. Rev.* 1999, 99, 1643; b) J. C. Chambron, J.-P. Sauvage, *Chem. Eur. J.* 1998, 4, 1362; c) J.-P. Sauvage, *Acc. Chem. Res.* 1998, 31, 611.
- [5] a) S. S. Zhu, T. M. Swager, *J. Am. Chem. Soc.* 1996, 118, 8713; b) S. S. Zhu, T. M. Swager, *J. Am. Chem. Soc.* 1997, 119, 12568.
- [6] S. S. Zhu, T. M. Swager, *Adv. Mater.* 1996, 8, 497.
- [7] P. L. Vidal, M. Billon, B. Divisia-Blohorn, G. Bidan, J. M. Kern, J.-P. Sauvage, *Chem. Commun.* 1998, 629.

- [8] a) G. P. Kittlesen, H. S. White, M. S. Wrighton, *J. Am. Chem. Soc.* **1984**, *106*, 7389; b) J. W. Thackeray, H. S. White, M. S. Wrighton, *J. Phys. Chem.* **1985**, *89*, 5133.
- [9] S. S. Zhu, R. P. Kingsborough, T. M. Swager, *J. Mater. Chem.* **1999**, *9*, 2123–2134.
- [10] All calculations were performed with the Spartan program (Wavefunction, Inc.). The geometry of **1** was optimized using semiempirical calculations (PM3). The structure of the octamer was minimized by molecular mechanics (MMFF94).
- [11] To obtain conductivities the coverage on the electrodes were determined by profilometry and are related to that of poly(3-methylthiophene),  $\sigma = 60 \text{ S cm}^{-1}$  to correct for non-uniform coverage. This method has been established to provide a reliable measurement of a number of electropolymerizable monomers.<sup>[12, 13]</sup>
- [12] R. P. Kingsborough, T. M. Swager, *Adv. Mater.* **1998**, *10*, 1100.
- [13] a) G. Zotti, G. Schiavon, *Synth. Met.* **1990**, *39*, 183; b) G. Schiavon, S. Sitran, G. Zotti, *Synth. Met.* **1989**, *32*, 209.
- [14] Q. Zhou, T. M. Swager, *J. Am. Chem. Soc.* **1995**, *117*, 12593.
- [15] C. O. Dietrich-Buchecker, J.-P. Sauvage, *Tetrahedron Lett.* **1983**, *24*, 5091.

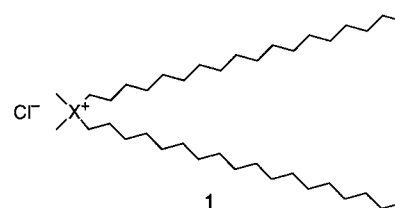
## Polar Thin Films Produced by Phosphonium Liquid Crystals: Two-Dimensional Self-Assembled Ionic Layers with Spontaneous Polarization\*\*

Akihiko Kanazawa, Tomiki Ikeda,\* and Jiro Abe

The area of thin film assemblies that have layer structures is rapidly developing into a key technology with applications ranging from chemical sensor systems to electronic materials (dielectrics, semiconductors, superconductors, optoelectronics, magnetic substances, and so forth).<sup>[1]</sup> The layered thin films are usually prepared from organic or inorganic materials by a variety of physical and chemical techniques (including, among others, laser ablation, evaporation, sputtering, chemical vapor deposition, the Langmuir–Blodgett technique, and sol–gel processing).<sup>[1a,b, 2]</sup> For solid-state thin films, however, it is often difficult to control the layer structure and the molecular (or atomic) arrangement. Since crystalline materials are mainly used as sources for the thin film assemblies, the assembly structures are limited by the intrinsic single-crystal structures of these sources. Clearly, the ability to control of organizational structure at the molecular or atomic levels is very important in development of new functionalized materials. Recently, supramolecular assemblies have been regarded as one of the most promising systems for applications in highly functionalized materials.<sup>[3]</sup> Liquid-crystalline materials have self-assembly characteristics for forming various phases and

provide additional features such as the ability to respond to applied external fields. The assembly structures are directed by the choice of phase, so that the structurally controlled thin films could be prepared by quenching from the appropriate fluid phase into the solid state.<sup>[4]</sup> The incorporation of the liquid-crystalline properties into layered materials may be expected to bring about emergence of more functionalized thin films with characteristic structural features.

Through systematic studies on the applications of ionic amphiphiles to multifunctional materials (for example: antimicrobial agents, surfactants, phase-transfer catalysts, anti-static agents, ion exchangers, curing agents), we found that phosphonium salts, which are composed of an ion pair of positive phosphorus and negative halide atoms as well as two long alkyl segments, **1** (X = P), possess a high degree of molecular organization abilities in comparison with the common quaternary ammonium analogs, **1** (X = N), with the same structure except for the positively charged heteroatom.<sup>[5]</sup>



Even in the bulk state, the phosphonium salts showed an advantageous feature as a thermotropic liquid crystal in spite of being structurally simple amphiphiles.<sup>[5c, 6]</sup> These salts formed a multilayer structure based on the bilayer stacking of the smectic A phase, which is built up from alternating layers of ions and alkyl segments. If such ionic liquid crystals are applied to solid-state systems, they may be regarded as a novel class of layered thin films because of the presence of two-dimensional polar layers, which are composed of pairs of positive and negative ions forming an electric dipole, separated by the insulating alkyl layers. Here we present unique feature of self-assembled layered thin films produced by the phosphonium liquid crystals, which was revealed through the evaluation of the second-order nonlinear optical properties (Figure 1).

To determine the spatial arrangement of ions in the layers the second-harmonic generation (SHG) was measured, which is an effective tool for evaluation of dipolar alignment in the molecular organizations. For the SHG measurement, we used the thermotropic liquid-crystalline phosphonium chloride (P-LC) and the quaternary ammonium analog (N-LC) as a reference liquid crystal. Solid-state samples retaining a smectic layer structure were readily prepared by injecting the compounds into a sandwiching cell with a gap of 15  $\mu\text{m}$  in the isotropic phase, followed by rapid cooling to room temperature. These samples were colorless and transparent. Figure 2 shows changes in the SHG intensity observed for the P-LC and the N-LC films. The polarized exciting beam was introduced along the  $z$  axis (Figure 1b). Second-harmonic generating signals were clearly observed for P-LC (Figure 2a). On the other hand, N-LC with the same hydrophobic structure was SHG-inactive (Figure 2b). These results indicate that the second-order nonlinear optical response of the

[\*] Prof. Dr. T. Ikeda, Dr. A. Kanazawa  
 Research Laboratory of Resources Utilization  
 Tokyo Institute of Technology  
 4259 Nagatsuta, Midori-ku, Yokohama 226-8503 (Japan)  
 Fax: (+81)45-924-5275  
 E-mail: tikeda@res.titech.ac.jp  
 Dr. J. Abe  
 Faculty of Engineering, Tokyo Institute of Polytechnics  
 1583 Iiyama, Atsugi 243-0297 (Japan)

\*\*] We thank Makoto Ogura and Atsuya Takahashi of Fujitsu, Ltd., and Azuma Matsuura and Tomoaki Hayano of Fujitsu Laboratories, Ltd., for the use of the latest version of the ANCHOR II system.<sup>[14]</sup>